Dynamics of dc bus networks and their stabilization by decentralized delayed feedback

Dynamics of dc bus networks and their stabilization by decentralized delayed feedback

Keiji Konishi,* Yoshiki Sugitani, and Naoyuki Hara
Department of Electrical and Information Systems, Osaka Prefecture University, 1-1 Gakuen-cho, Naka-ku, Sakai, Osaka 599-8531, Japan
(Received 7 October 2014; published 15 January 2015)

The present paper deals with the dynamics of bus networks, which consist of several identical dc bus systems connected by resistors. It is analytically guaranteed that the stability of a stand-alone dc bus system is equivalent to that of the networks, independent of the number of bus systems and the network topology. In addition, we show that a decentralized delayed-feedback control can stabilize an unstable operating point embedded within the networks. Moreover, this stabilization does not depend on the number of bus systems or the network topology. A systematic procedure for designing the controller is presented. Finally, the validity of the analytical results is confirmed through numerical examples.

DOI: 10.1103/PhysRevE.91.012911 PACS number(s): 05.45.Xt, 05.45.Ra, 05.45.Gg, 89.75.−k

I. INTRODUCTION

In recent years, there has been growing interest in the behavior of power-grid networks from academic and industrial viewpoints [1–5]. Networks can be classified into two types: alternating-current (ac) networks and direct-current (dc) networks [6]. With the recent increases in dc loads, dc generation, and dc storage thanks to recent progress in power electronics, dc bus systems are widely expected to play an important part in future electronic power systems [6]. Unfortunately, the dc bus system has a serious drawback, namely the bus line voltage has the potential to be unstable if constant power loads (CPLs), which continuously consume the same amount of power, are connected to the bus line. Note that a number of present and future power loads will be CPLs [7]. Therefore, it is strongly desired to overcome the above-described drawback in power electronics. A number of investigations have been conducted to analyze and overcome this drawback from the viewpoints of power electronics [8–15]. However, few studies have investigated this drawback from the viewpoint of nonlinear dynamics.

In a previous study, we demonstrated that bifurcation theory analytically clarifies the dynamics of a simplified dc bus system [16]. Furthermore, a delayed-feedback control [17] was used to overcome the drawback regarding potential instability. The application of a delayed-feedback control to the simplified dc bus system allows us to noninvasively stabilize an unstable operating point without using the location of the point. In addition, the stability of the operating point is maintained by a small control signal even when a system parameter (e.g., the consumption power of the CPL) is varied very slowly. Although our previously proposed method would seem to be a candidate for overcoming the above-mentioned drawback, it can be used only in a simplified stand-alone dc bus system. However, in real situations, bus systems consist of *multiple* power sources and loads [18–22], which suggests that the previously proposed method cannot be used in such real situations.

The present paper analytically investigates the dynamics of bus networks, which consist of several identical dc bus systems connected by resistors (see Fig. 1). We show that some features of the Laplacian matrix simplify the stability analysis of a spatially uniform operating point. The analytical results on stability are numerically confirmed using a bus network, the topology and coupling strength of which are sequentially switched. In addition, numerical simulations are performed for more practical situations, in which each bus system has different parameters. Furthermore, we apply a decentralized delayed-feedback control [23] to dc bus networks to stabilize a spatially uniform *unstable* operating point. The systematic procedure for designing the controller parameters is provided. The main advantage of this controller is that the designed controller stabilizes the *unstable* operating point independently of its network topology and coupling strength. The performance of the designed controller for bus networks is confirmed through numerical simulations.

II. DC BUS NETWORKS

This section considers dynamic behavior of bus networks. First, the circuit equation of bus networks will be transformed into simple dimensionless dynamical systems. Second, the stability of spatially uniform equilibrium, i.e., the operating point, will be analytically investigated. Finally, the validity of the analytical results will be confirmed through numerical simulations.

A. Dynamical systems

Let us consider the dc bus network illustrated in Fig. 1. Each bus system has a dc voltage source with voltage E, resistance R, inductance L, and capacitance C. The source supplies the electric power to its load (i.e., CPL). These bus systems are coupled by the connection resistance r. The voltage and current of bus system n are denoted by $v_n(t)$ and $i_n(t)$, respectively. Note that their product, the consumed power, is always constant as $P = v_n(t)i_n(t)$ for any $t \geqslant 0$ and for any $n \in \{1, \ldots, N\}$, where N is the number of bus systems.

The circuit equation of a bus network is described as follows:

$$\begin{aligned} C\frac{dv_n(t)}{dt} &= -\frac{P}{v_n(t)} + i_n(t) + \frac{1}{r}\sum_{m=1}^{N} c_{nm}\{v_m(t) - v_n(t)\}, \\ L\frac{di_n(t)}{dt} &= -v_n(t) - Ri_n(t) + E, \end{aligned} \tag{1}$$

*http://www.eis.osakafu-u.ac.jp/∼ecs

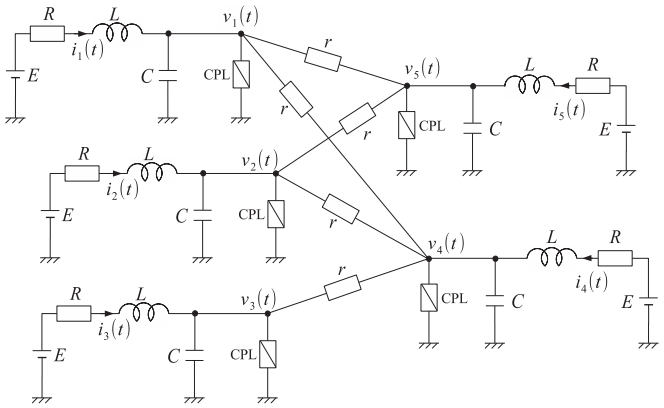

FIG. 1. Schematic diagram of a dc bus network.

for $n = 1,\ldots,N$. Here c_{nm} represents the network topology. If system n is connected to system m with a connection resistance r, then $c_{nm} = c_{mn} = 1$, otherwise $c_{nm} = c_{mn} = 0$. Furthermore, we have $c_{nn} = 0$. The transformation of system variables, time, and parameters, i.e.,

$$x_n := \frac{1}{E}v_n(t), \quad y_n := \frac{L}{CRE}i_n(t), \quad \tau := \frac{t}{RC}, \\ a := \frac{PR}{E^2}, \quad b := \frac{R^2}{L/C}, \quad \varepsilon := \frac{R}{r}, \tag{2}$$

allows us to reduce the circuit equation of Eq. (1) to a dimensionless model:

$$\dot{x}_n = -\frac{a}{x_n} + by_n + u_n^{(\varepsilon)}, \\ \dot{y}_n = -x_n - by_n + 1, \tag{3}$$

where the connection signal is described by

$$u_n^{(\varepsilon)} := \varepsilon\sum_{m=1}^{N} c_{nm}(x_m - x_n). \tag{4}$$

Note that dimensionless model (3) is suitable for the investigation of dynamics from the viewpoint of nonlinear dynamics, because the six circuit parameters (R,L,C,r,E,P) in circuit equation (1) are reduced to three parameters (a,b,ε).

Each bus system (3) without connection (i.e., $\varepsilon \equiv 0$) has two fixed points, $\boldsymbol{p}_+ := [x_+^*, y_+^*]^T$ and $\boldsymbol{p}_- := [x_-^*, y_-^*]^T$, where

$$x_\pm^* = \frac{1}{2}(1 \pm \sqrt{1-4a}), \quad y_\pm^* = \frac{a}{bx_\pm^*}.$$

Note that bus network (3) with a connection (i.e., $\varepsilon > 0$) has two spatially uniform equilibrium states:

$$\boldsymbol{X}_\pm^* = [\boldsymbol{p}_\pm^T\ \boldsymbol{p}_\pm^T \cdots \boldsymbol{p}_\pm^T]^T.$$

The error states from these equilibrium states, i.e.,

$$\boldsymbol{X} := [x_1\ y_1 \cdots x_N\ y_N]^T - \boldsymbol{X}_\pm^*, \tag{5}$$

are governed by the linear system,

$$\dot{\boldsymbol{X}} = [\boldsymbol{I}_N \otimes \boldsymbol{A}(x_\pm^*) - \varepsilon\boldsymbol{L} \otimes \boldsymbol{J}]\boldsymbol{X}, \tag{6}$$

where

$$\boldsymbol{A}(x_\pm^*) := \begin{bmatrix} a/(x_\pm^*)^2 & b \\ -1 & -b \end{bmatrix}, \quad \boldsymbol{J} := \begin{bmatrix} 1 & 0 \\ 0 & 0 \end{bmatrix}.$$

Here $\boldsymbol{I}_N$ is the N-dimensional unit matrix. $\boldsymbol{L}$ is the Laplacian matrix $\boldsymbol{L} = \{L_{nm}\} := \boldsymbol{D} - \boldsymbol{C}$ with the adjacency matrix $\boldsymbol{C} = \{c_{nm}\}$ and with the degree matrix $\boldsymbol{D} = \mathrm{diag}(d_1,\ldots,d_N)$, $d_n = \sum_{m=1}^{N} c_{nm}$. Moreover, $\boldsymbol{A}(x_\pm^*)$ denotes the Jacobi matrix for each bus system (3) without a connection at the fixed point $\boldsymbol{p}_\pm$. The stability of $\boldsymbol{p}_\pm$ is equivalent to that of matrix $\boldsymbol{A}(x_\pm^*)$. Note that the stability of equilibrium state $\boldsymbol{X}_+^*$ ($\boldsymbol{X}_-^*$) is equivalent to that of linear system (6) with $\boldsymbol{A}(x_+^*)$ ($\boldsymbol{A}(x_-^*)$).

B. Stability analysis

In this subsection, we analyze the stability of the equilibrium states $\boldsymbol{X}_\pm^*$. The Laplacian matrix $\boldsymbol{L}$ is a real symmetric matrix. Then there exists a diagonal transformation matrix $\boldsymbol{T}$ such that $\boldsymbol{T}^{-1}\boldsymbol{L}\boldsymbol{T} = \mathrm{diag}(\lambda_1,\ldots,\lambda_N)$. Note that the eigenvalues of $\boldsymbol{L}$, λ_i $(i = 1,\ldots,N)$, always satisfy the following [24]:

$$0 = \lambda_1 \leqslant \lambda_2 \leqslant \cdots \leqslant \lambda_N. \tag{7}$$

Define a new variable $\boldsymbol{Z} = [\boldsymbol{z}_1^T \cdots \boldsymbol{z}_N^T]^T := (\boldsymbol{T} \otimes \boldsymbol{I}_2)^{-1}\boldsymbol{X}$ so linear system (6) can be rewritten as

$$\dot{\boldsymbol{Z}} = (\boldsymbol{T} \otimes \boldsymbol{I}_2)^{-1}[\boldsymbol{I}_N \otimes \boldsymbol{A}(x_\pm^*) - \varepsilon\boldsymbol{L} \otimes \boldsymbol{J}](\boldsymbol{T} \otimes \boldsymbol{I}_2)\boldsymbol{Z} \\ = [\boldsymbol{I}_N \otimes \boldsymbol{A}(x_\pm^*) - \varepsilon\mathrm{diag}(\lambda_1,\ldots,\lambda_N) \otimes \boldsymbol{J}]\boldsymbol{Z}. \tag{8}$$

Since linear system (8) is diagonalized, we see that this system is stable if and only if all of the following systems are stable:

$$\dot{\boldsymbol{z}}_i = [\boldsymbol{A}(x_\pm^*) - \varepsilon\lambda_i\boldsymbol{J}]\boldsymbol{z}_i, \ (i = 1,\ldots,N). \tag{9}$$

This fact leads us to obtain the following lemma.

Lemma 1. The spatially uniform equilibrium state $\boldsymbol{X}_-^*$ of bus network (3) cannot be stabilized for any topology $\boldsymbol{L}$ and any coupling strength $\varepsilon > 0$. Furthermore, if the fixed point $\boldsymbol{p}_+$ of bus system (3) without a connection ($\varepsilon \equiv 0$) is unstable, the state $\boldsymbol{X}_+^*$ cannot be stabilized for any topology $\boldsymbol{L}$ and any coupling strength $\varepsilon > 0$.

Proof. From $\lambda_1 = 0$ in Eq. (7), systems (9) include $\dot{\boldsymbol{z}}_1 = \boldsymbol{A}(x_\pm^*)\boldsymbol{z}_1$, which does not depend on $\boldsymbol{L}$ and ε. This suggests that if $\boldsymbol{A}(x_\pm^*)$ is unstable, then the state $\boldsymbol{X}_\pm^*$ is unstable for any $\boldsymbol{L}$ and for any ε. Since $\boldsymbol{A}(x_-^*)$ is always unstable [16], the state $\boldsymbol{X}_-^*$ is unstable, independent of $\boldsymbol{L}$ and ε. Furthermore, note that if $\boldsymbol{A}(x_+^*)$ is unstable, the state $\boldsymbol{X}_+^*$ is unstable, independent of $\boldsymbol{L}$ and ε. ■

Lemma 1 restricts our attention to dynamics around the state $\boldsymbol{X}_+^*$. Thus, the present paper will deal only with the dynamics of systems (9) with $\boldsymbol{A}(x_+^*)$,

$$\dot{\boldsymbol{z}}_i = [\boldsymbol{A}(x_+^*) - \varepsilon\lambda_i\boldsymbol{J}]\boldsymbol{z}_i, \\ = \begin{bmatrix} a^* - \varepsilon\lambda_i & b \\ -1 & -b \end{bmatrix}\boldsymbol{z}_i, \ (i = 1,\ldots,N), \tag{10}$$

where the parameter a^* is given by

$$a^* := \frac{a}{(x_+^*)^2} = \frac{4a}{(1+\sqrt{1-4a})^2}. \tag{11}$$

Systems (10) yield the following.

Theorem 1. The spatially uniform equilibrium state $\boldsymbol{X}_+^*$ of bus network (3) is stable for any topology $\boldsymbol{L}$ and any coupling strength $\varepsilon > 0$ if and only if the fixed point $\boldsymbol{p}_+$ of bus system (3) without connection ($\varepsilon \equiv 0$) is stable.

Proof. The characteristic polynomial of system i in Eq. (10) is given by $h(s,\lambda_i) = s^2 + a_1(\lambda_i)s + a_0(\lambda_i)$, where $a_1(\lambda_i) := b - a^* + \varepsilon\lambda_i$ and $a_0(\lambda_i) := b(1 - a^* + \varepsilon\lambda_i)$. The necessary and sufficient condition for $h(s,\lambda_i)$ to be stable is that both $a_1(\lambda_i) > 0$ and $a_0(\lambda_i) > 0$ hold. By simple manipulation, this condition can be rewritten as follows:

$$a^* - \varepsilon\lambda_i < \min\{1,b\}. \tag{12}$$

From inequality (12) with condition (7), the stability of $\boldsymbol{X}_+^*$ is equivalent to that of $\boldsymbol{p}_+$, independent of $\boldsymbol{L}$ and $\varepsilon > 0$. ■

Theorem 1 guarantees that the stability of the operating point $\boldsymbol{p}_+$ in each stand-alone bus system remains even if the systems are coupled by the connection resistance. Therefore, it can be concluded that, for $\boldsymbol{X}_+^*$ to be stable independent of the network topology and the connection resistance, we need only design the parameters a and b in accordance with our previous paper [16], such that $\boldsymbol{p}_+$ in each stand-alone bus system is stable.

C. Numerical examples

In this subsection, we confirm the validity of the analytical results through numerical simulations. Let us consider five different bus networks, as illustrated in Fig. 2. The parameters a and b are fixed such that $\boldsymbol{p}_+$ in a stand-alone bus system is stable: $a = 0.10$ and $b = 0.20$ [16]. Figure 3 shows the time-series data for x_n and $u_n^{(\varepsilon)}$ in a bus network for which the topology and coupling strength are sequentially switched from Network 0 to Network 4. Note that all of the system states (x_n, y_n) are randomly changed with small amplitude 0.03 at every instance of switching because such perturbations are required in order to confirm the stability of $\boldsymbol{X}_+^*$ through numerical simulations. All x_n and $u_n^{(\varepsilon)}$ converge on $x_+^* = 0.8873$ and 0, respectively. Thus, we may say that this numerical result supports Theorem 1.

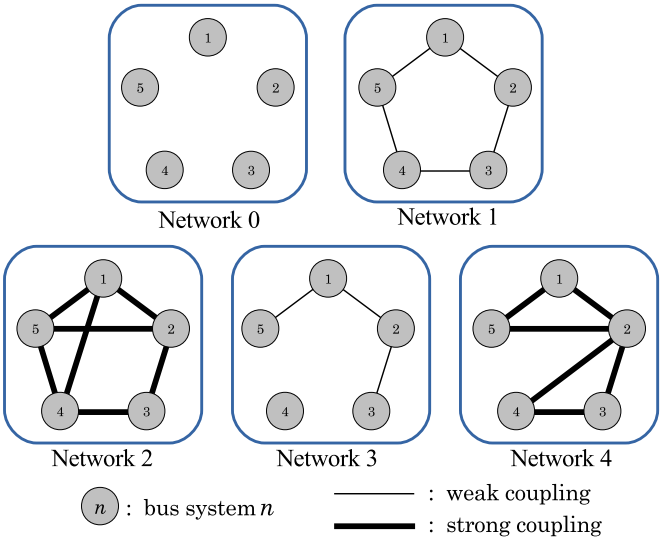

FIG. 2. (Color online) Five different bus networks: Network 0 (no connection), Network 1 (ring network on weak coupling), Network 2 (ring network with two shortcuts on strong coupling), Network 3 (chain network on weak coupling), and Network 4 (network 3 with bus system 4 on strong coupling).

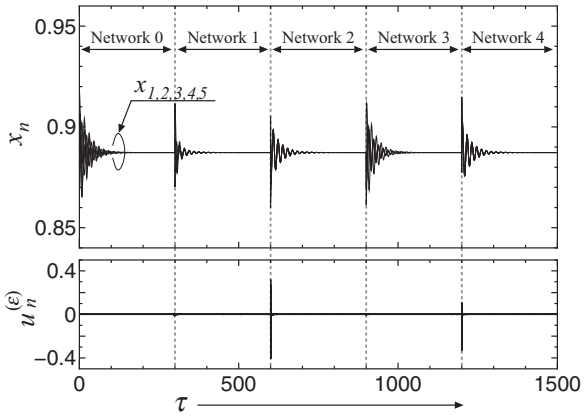

FIG. 3. Time-series data for x_n and $u_n^{(\varepsilon)}$ $(n = 1, \ldots, 5)$ in a bus network for which the topology and coupling strength are sequentially switched from Network 0 to Network 4: $\varepsilon = 0.1$ for Networks 1 and 3 and $\varepsilon = 1.0$ for Networks 2 and 4.

Note that the numerical results were obtained under the assumption that the parameters (a,b,ε) in each bus system are identical. Although this assumption simplifies the analysis, it is not practical for real bus networks. Next we consider two situations in which (a) all of the bus systems have different parameters with a margin of $\pm p \times 100\%$ errors and (b) one of bus systems has an extremely large a (i.e., the stand-alone bus system has an unstable $\boldsymbol{p}_+$), whereas the other bus systems have a small a (i.e., the others have a stable $\boldsymbol{p}_+$).

For situation (a), the parameters a_n, b_n, and ε_n of system n are randomly chosen from among $a_n \in [(1-p)\bar{a},(1+p)\bar{a}], b_n \in [(1-p)\bar{b},(1+p)\bar{b}], \varepsilon_n \in [(1-p)\bar{\varepsilon},(1+p)\bar{\varepsilon}]$, where $(\bar{a},\bar{b},\bar{\varepsilon})$ are the nominal values. Figure 4 shows the parameter region of stable spatially uniform equilibrium state $\boldsymbol{X}_+^*$ with parameters mismatch $p = 0.2$ (20%). The gray region indicates the nominal parameter set $(\bar{a},\bar{b})$ where a bus network does not diverge even when its topology and coupling strength are sequentially switched as

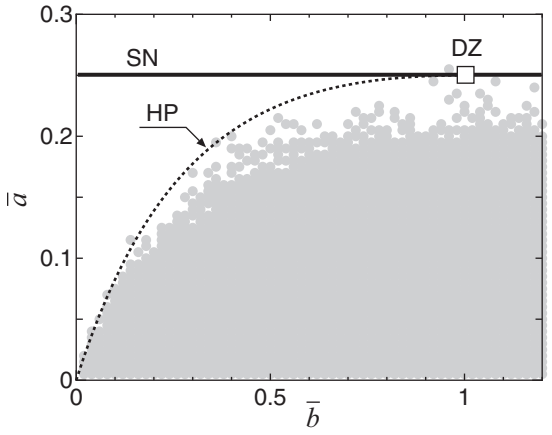

FIG. 4. Parameter region of stable, spatially uniform equilibrium state $\boldsymbol{X}_+^*$ with parameter mismatch $p = 0.2$ (20%). Gray region: $(\bar{a},\bar{b})$, where a bus network switched as shown in Fig. 3 does not diverge. HP, Hopf bifurcation; SN, saddle-node bifurcation; DZ, double-zero bifurcation.

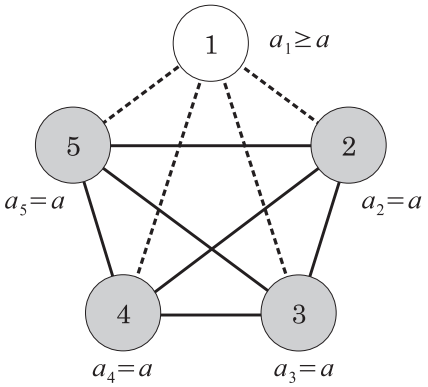

FIG. 5. Schematic diagram of a bus system network: system 1 has a high CPL $a_1 > a_{\rm HP}$ and the other systems have low CPLs $a_2 = a_3 = a_4 = a_5 < a_{\rm HP}$. All of the bus systems have $b_1 = \cdots = b_5 < 1$.

shown in Fig. 3. According to our previous result [16], for no parameter mismatch $p = 0$, a stand-alone bus system has stable $\boldsymbol{p}_+$ if $a < a_{\rm HP}$ for $b \leqslant 1$ and $a < a_{\rm SN}$ for $b \geqslant 1$, where $a_{\rm HP}$ and $a_{\rm SN}$ denote the Hopf (HP) and saddle-node (SN) bifurcation points, respectively. The region with parameter mismatch shrinks in comparison with the region with no parameter mismatch. This is because for a nominal parameter set $(\bar{a},\bar{b})$ just below bifurcation curves, some buses can have the parameter set (a_n,b_n) above the curves due to random choice. On the other hand, this numerical result suggests that our previous result [16] is useful for design of the nominal parameters $(\bar{a},\bar{b},\bar{\varepsilon})$ such that the bus system networks are stable even with some parameter mismatch.

For situation (b), as shown in Fig. 5, we assume that bus system 1 has a high CPL, $a_1 > a_{\rm HP} = 5/36$, and that the other systems have low CPLs, $a_2 = a_3 = a_4 = a_5 = 0.1 < a_{\rm HP}$. The other parameters are set to $b_1 = \cdots = b_5 = 0.2$ and $\varepsilon_1 = \cdots = \varepsilon_5 = 0.05$. Furthermore, all of the bus systems except system 1 are completely connected (i.e., all-to-all connection: see the solid lines in Fig. 5), and bus system 1 is connected to some of the systems (see the dotted lines in Fig. 5). Now let us consider the network behavior through numerical simulations. Figure 6 shows the time-series data of x_n with a step-by-step increase of a_1. Bus system 1 is connected only to system 2. In order to numerically investigate the stability, all of the states are randomly disturbed with small amplitude 0.03 at instances when a_1 jumps to the next higher level. As can be seen, x_1 decreases with an increase in a_1, and all the states converge on their operating points, even with the random disturbance. All of the states eventually diverge when a_1 reaches $\hat{a}_1$. Note that the network system is stable for any $a_1 \in [a_{\rm HP},\hat{a}_1]$. This suggests that stand-alone bus system 1, which has an unstable fixed point, can be stabilized with the help of the other stable bus systems. In other words, we may say that all of the bus systems behave cooperatively.

In order to investigate the cooperative effect of the coupling strength ε and the degree of system 1 (i.e., the number of connections to system 1: $d_1 := \sum_{n=1}^{N} c_{1n}$) on stability of the network, we numerically estimate the critical parameter value $\hat{a}_1$ (see Fig. 6), under which the network system does not diverge, with respect to ε and d_1, as shown in Fig. 7. The critical parameter value $\hat{a}_1$ increases as ε and d_1 increase. For small

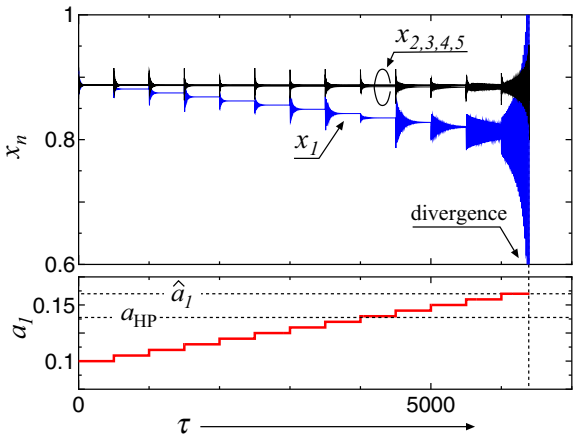

FIG. 6. (Color online) Time-series data of states x_n $(n = 1,\ldots,5)$ and parameter a_1 for the bus system network shown in Fig. 5 ($a_2 = \cdots = a_5 = 0.1 < a_{\rm HP} = 5/36$, $b_1 = \cdots = b_5 = 0.2 < 1$, $\varepsilon_1 = \cdots = \varepsilon_5 = 0.05$). All of the states are randomly disturbed with small amplitude 0.03 at instances when a_1 jumps to the next higher level. Bus system 1 is connected only to system 2.

ε, the critical value $\hat{a}_1$ is between $a_{\rm HP}$ and $a_{\rm SN}$, which implies that the unstable operating point of system 1 is stabilized due to the connections to the stable bus systems. For large ε, $\hat{a}_1$ exceeds $a_{\rm SN}$, i.e., the stable operating point of system 1 is induced by such a connection. This result demonstrates that the cooperative performance can be enhanced by using high ε and d_1.

III. STABILIZATION OF DC BUS NETWORKS

This section will show that unstable $\boldsymbol{X}^*_+$ in bus networks can be stabilized by a decentralized delayed-feedback control. A systematic procedure for designing the controller is provided. The performance of the designed controller is examined through numerical simulations.

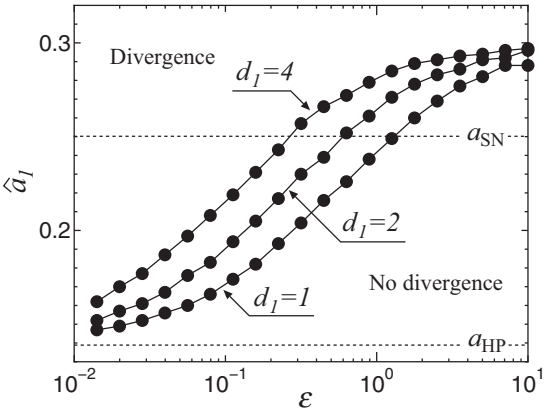

FIG. 7. Critical parameter value $\hat{a}_1$ as a function of coupling strength ε and the degree of system 1, d_1. The parameters and the numerical procedure are the same as in Fig. 6.

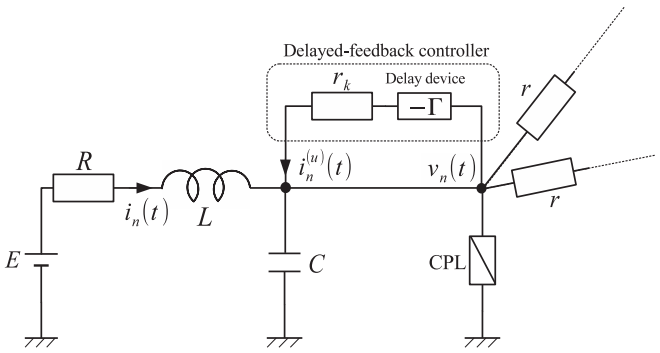

FIG. 8. Schematic diagram of a dc bus system with delayed feedback

A. Decentralized delayed feedback

Let us review the analytical results for a stand-alone bus system (3) with $r \equiv +\infty$ (i.e., $\varepsilon \equiv 0$) [16]. For an impedance $\sqrt{L/C}$ of less than R (i.e., $b < 1$), an increase in the consumption of the load P (i.e., large a) causes the stable fixed point $\boldsymbol{p}_+$ to become unstable via the Hopf bifurcation.

Lemma 1 suggests that if stand-alone bus systems have such unstable $\boldsymbol{p}_+$, the spatially uniform equilibrium state $\boldsymbol{X}_+^*$ in bus networks must be unstable. This situation indicates that the power sources cannot supply electric power to the loads in networks. In order to avoid such a supply problem, we will attempt to stabilize the unstable $\boldsymbol{X}_+^*$.

The decentralized delayed-feedback control,[1] an extended version of a popular delayed-feedback control [17,25] for stabilizing unstable periodic orbits [26,27] and unstable fixed points [28,29] in chaotic systems, will be applied to each bus system in networks, as shown in Fig. 8. Circuit equation (1) with control current $i_n^{(u)}(t)$, which is injected from the delayed-feedback controller to the bus system, is described as follows:

$$C\frac{dv_n(t)}{dt} = -\frac{P}{v_n(t)} + i_n(t) + \frac{1}{r}\sum_{m=1}^{N} c_{nm}\{v_m(t) - v_n(t)\} + i_n^{(u)}(t),$$

$$L\frac{di_n(t)}{dt} = -v_n(t) - Ri_n(t) + E,$$

where $i_n^{(u)}(t)$ is given by

$$i_n^{(u)}(t) = \frac{1}{r_k}\{v_n(t-\Gamma) - v_n(t)\}.$$

Here $v_n(t-\Gamma)$ represents the past bus voltage in bus system n with delay time $\Gamma \geqslant 0$. Transformations (2) and

$$x_{n,T} := \frac{1}{E}v_n(t-\Gamma), \quad T := \frac{\Gamma}{RC}, \quad k := \frac{R}{r_k},$$

yield a dimensionless model,

$$\dot{x}_n = -\frac{a}{x_n} + by_n + u_n^{(\varepsilon)} + u_n^{(k)},$$
$$\dot{y}_n = -x_n - by_n + 1, \tag{13}$$

where the control signal is given by

$$u_n^{(k)} := k(x_{n,T} - x_n). \tag{14}$$

We use delayed-feedback controller (14) for the following reasons. The control signal $u_n^{(k)}$ for maintaining the stable state $\boldsymbol{X}_+^*$ is zero due to its noninvasive property. The location of $\boldsymbol{X}_+^*$ in networks never moves for any network topology and any connection resistance, even if controller (14) works.

For now, we investigate the stability of $\boldsymbol{X}_+^*$ in networks consisting of dimensionless models (13) with controllers (14). Define an error state by Eq. (5) and

$$\boldsymbol{X}_T := [x_{1,T}\ y_{1,T} \cdots x_{N,T}\ y_{N,T}]^T - \boldsymbol{X}_+^*,$$

so the dynamics around $\boldsymbol{X}_+^*$ takes the form

$$\dot{\boldsymbol{X}} = [\boldsymbol{I}_N \otimes \{\boldsymbol{A}(x_+^*) - k\boldsymbol{J}\} - \varepsilon\boldsymbol{L} \otimes \boldsymbol{J}]\boldsymbol{X} + [\boldsymbol{I}_N \otimes (k\boldsymbol{J})]\boldsymbol{X}_T. \tag{15}$$

Using the variables $\boldsymbol{Z}$ defined in the preceding section and $\boldsymbol{Z}_T := (\boldsymbol{T} \otimes \boldsymbol{I}_2)^{-1}\boldsymbol{X}_T$, we rewrite linear system (15) as

$$\dot{\boldsymbol{Z}} = [\boldsymbol{I}_N \otimes \{\boldsymbol{A}(x_+^*) - k\boldsymbol{J}\} - \varepsilon\mathrm{diag}(\lambda_1, \ldots, \lambda_N) \otimes \boldsymbol{J}]\boldsymbol{Z} + [\boldsymbol{I}_N \otimes (k\boldsymbol{J})]\boldsymbol{Z}_T.$$

Since this system is diagonalized, the necessary and sufficient condition for this system to be stable is that all

$$\dot{z}_i = \begin{bmatrix} a^* - \varepsilon\lambda_i - k & b \\ -1 & -b \end{bmatrix} z_i + \begin{bmatrix} k & 0 \\ 0 & 0 \end{bmatrix} z_{i,T}, \ (i = 1, \ldots, N), \tag{16}$$

be stable, where $z_{i,T} := z_i(\tau - T)$. The characteristic quasipolynomial of linear systems (16) is given by

$$G(s,T) = \prod_{i=1}^{N} g(s,T,\varepsilon\lambda_i), \tag{17}$$

where

$$g(s,T,\Delta\gamma) := s^2 + (b - a^*)s + b(1 - a^*) + (s + b)\{\Delta\gamma + k(1 - e^{-sT})\}. \tag{18}$$

We see that if $g(s,T,\Delta\gamma)$ is stable for any $\Delta\gamma \in [0,\varepsilon\hat{\lambda}]$, then the state $\boldsymbol{X}_+^*$ is guaranteed to be stable for any $\boldsymbol{L}$, the maximum real eigenvalue λ_N of which is less than or equal to $\hat{\lambda}$. Remark that a quasipolynomial is said to be stable if and only if all its roots are in the open left half of the complex plane.

B. Design of the controller

In this subsection, we present a systematic procedure for designing the feedback gain $k > 0$ and the delay time $T > 0$ such that the state $\boldsymbol{X}_+^*$ becomes stable[2] for any $\boldsymbol{L}$ and any

[1]The decentralized delayed-feedback control for coupled map lattices was proposed in our previous study [23], whereas that for continuous-time networks, to the best of our knowledge, has not been proposed in the field of nonlinear science and control.

[2]Note that there is no upper bound for $\varepsilon \geqslant 0$ and $\lambda_N \geqslant 0$, because we do not restrict the value of r, the number N, or the network topology $\boldsymbol{L}$.

$\varepsilon > 0$. This can be reduced to the problem of designing $k > 0$ and $T > 0$ such that $g(s,T,\Delta\gamma)$ is stable for any $\Delta\gamma \geqslant 0$.

Here recall that our previous study [16] provided a systematic procedure for designing $k > 0$ and $T > 0$ such that the unstable fixed point $\boldsymbol{p}_+$ in a stand-alone bus system, the characteristic quasipolynomial of which is given by $g(s,T,0)$, becomes stable as follows.

Theorem 2 (Refs. [16,30]). Consider $g(s,T,0)$, characteristic quasipolynomial (18) with $\Delta\gamma = 0$, under the assumption

$$b < a^* < 1. \tag{19}$$

If k satisfies all of the inequalities,

$$\begin{aligned} d_1 &:= b^2 + a^{*2} - 2b - 2a^*k < 0, \\ d_2 &:= d_1^2 - 4b^2(1-a^*)(1-a^*+2k) > 0, \\ d_3 &:= \frac{\psi_1}{\omega_1} - \frac{\psi_2}{\omega_2} < 0, \end{aligned} \tag{20}$$

where

$$\omega_1 := \sqrt{\frac{-d_1 - \sqrt{d_2}}{2}}, \quad \omega_2 := \sqrt{\frac{-d_1 + \sqrt{d_2}}{2}},$$

$$\psi_{1,2} := \mathrm{Arg}\left[\frac{k(b + j\omega_{1,2})}{b(1-a^*+k) - \omega_{1,2}^2 + j\omega_{1,2}(b-a^*+k)}\right],$$

then there exist T such that $g(s,T,0)$ is stable. In particular, $g(s,T,0)$ is stable if and only if T is within one of the intervals as follows:

$$\begin{aligned} T &\in \left(\frac{\psi_1 + 2\pi l}{\omega_1}, \frac{\psi_2 + 2\pi l}{\omega_2}\right), \\ l &= 0, \ldots, \left\lfloor \frac{\psi_2\omega_1 - \psi_1\omega_2}{2\pi(\omega_2 - \omega_1)} \right\rfloor, \end{aligned} \tag{21}$$

under condition (20). Here $\mathrm{Arg}[\mathsf{s}] \in [0, 2\pi)$ and $\lfloor \mathsf{r} \rfloor$ represent the principal argument of a complex number s and the largest integer not greater than r for a real number r, respectively. j represents the imaginary unit.

Inequality (19) is the necessary and sufficient condition for $\boldsymbol{A}(x_+^*)$ to have the two unstable eigenvalues. This condition indicates the situation in which the fixed point $\boldsymbol{p}_+$ in the stand-alone bus system is unstable. Furthermore, even though $g(s,T,0)$ with designed k and T is stable, we cannot guarantee the stability of $g(s,T,\Delta\gamma)$, which describes the stability of $\boldsymbol{X}_+^*$ in controlled bus networks. Thus, we present the following lemma.

Lemma 2. If there exist no $\omega \geqslant 0$ and $\Delta\gamma > 0$ such that, with k and T designed by Theorem 2, $g(j\omega,T,\Delta\gamma) = 0$ holds, then $g(s,T,\Delta\gamma)$ with the designed k and T is stable for any $\Delta\gamma > 0$. ■

Proof. Since $g(s,T,0)$ with k and T designed by Theorem 2 is stable, all of the roots of $g(s,T,0) = 0$ are within the open left half complex plane. The destabilization of $g(s,T,\Delta\gamma)$ for a given $\Delta\gamma > 0$ corresponds to the fact that at least one of the roots moves from left to right. Thus, if there exist no $\omega \geqslant 0$ and $\Delta\gamma > 0$ such that $g(j\omega,T,\Delta\gamma) = 0$ holds, no root of $g(s,T,\Delta\gamma) = 0$ moves from the left to the right for any $\Delta\gamma > 0$, which indicates that all of the roots of $g(s,T,0) = 0$ remain within the open left half complex plane for any $\Delta\gamma > 0$. ■

A simple procedure for checking the condition in Lemma 2 is provided below.

Lemma 3. For k and T designed by Theorem 2, if there exists no $\omega > 0$ such that both

$$f_1(\omega) := \omega^3 + \omega b(b-1) + k(b^2+\omega^2)\sin\omega T = 0, \tag{22}$$

$$f_2(\omega) := \omega(b-a^*) + \omega k(1-\cos\omega T) + bk\sin\omega T < 0, \tag{23}$$

hold, then $g(s,T,\Delta\gamma)$ is stable for any $\Delta\gamma \geqslant 0$.

Proof. The condition in Lemma 2 is equivalent to the fact that there exist no $\omega \geqslant 0$ and $\Delta\gamma > 0$ with the designed k and T such that

$$\begin{aligned} \frac{1}{b}\mathrm{Re}[g(j\omega,T,0)] &= -\Delta\gamma \\ \frac{1}{\omega}\mathrm{Im}[g(j\omega,T,0)] &= -\Delta\gamma, \end{aligned} \tag{24}$$

are satisfied. Note that, for $\omega = 0$, there exists no $\Delta\gamma$ satisfying Eq. (24). Thus, we need only consider $\omega > 0$. For common $\Delta\gamma > 0$ in the above two equations, the above fact can be reduced to the fact that there exists no $\omega > 0$ for

$$\omega\mathrm{Re}[g(j\omega,T,0)] = b\mathrm{Im}[g(j\omega,T,0)] < 0, \tag{25}$$

to be satisfied. The equality and the inequality in condition (25) are rewritten as Eq. (22) and inequality (23), respectively. Thus, if ω such that equality (22) and inequality (23) both hold does not exist, there exists no $\omega > 0$ satisfying condition (25). ■

Based on these lemmas, we can easily obtain our main result.

Theorem 3. Design k and T in controller (14) according to Theorem 2. If there exists no $\omega > 0$ such that both conditions (22) and (23) are satisfied, the state $\boldsymbol{X}_+^*$ in bus networks (13) with controllers (14) is stable for any topology $\boldsymbol{L}$ and any coupling strength $\varepsilon > 0$.

Proof. Since it is clear from Theorem 2 and Lemmas 2 and 3, this proof is omitted. ■

Corollary 1. For a given $a \equiv a_g$ and b, design k and T in controller (14) according to Theorem 3. Then the state $\boldsymbol{X}_+^*$ in bus networks (13) with controllers (14) is stable for any $a \in (0, a_g]$, any topology $\boldsymbol{L}$, and any coupling strength $\varepsilon > 0$.

Proof. Note that $g(s,T,\Delta\gamma)$ in Eq. (18) can be rewritten as

$$\begin{aligned} g(s,T,\Delta\gamma) := {} & s^2 + (b - a^* + \Delta\gamma)s + b(1 - a^* + \Delta\gamma) \\ & + k(s+b)(1 - e^{-sT}). \end{aligned} \tag{26}$$

Equation (11) suggests that a^* decreases monotonically with decreasing a for $a \in (0, 1/4)$. According to Eq. (26), a decrease in a is equivalent to an increase in $\Delta\gamma$. Since Lemma 3 guarantees the stability of $g(s,T,\Delta\gamma)$ for any $\Delta\gamma \geqslant 0$, it is obvious that, for a given $a \equiv a_g$, k and T designed by Theorem 3 are valid for any $a \in (0, a_g]$. ■

Now let us provide a systematic procedure for the design of k and T based on our analytical results.

Step 1: The parameters $a \equiv a_g$ and b are given, but the topology $\boldsymbol{L}$ and the coupling strength $\varepsilon > 0$ are unknown.

Step 2: Design k and T according to Theorem 2.

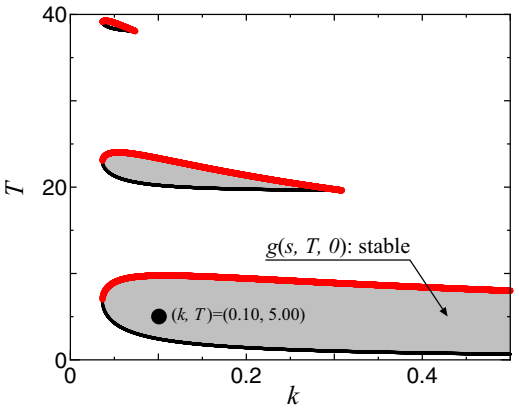

FIG. 9. (Color online) Boundary curves of T plotted with respect to k for $g(s,T,0)$ to be stable ($a = 0.17, b = 0.20$). Thin black (Bold red) line: lower (upper) stable intervals of T in Eq. (21).

Step 3: Plot $f_1(\omega)$ and $f_2(\omega)$ using the designed k and T. If there exists no $\omega > 0$ such that both $f_1(\omega) = 0$ and $f_2(\omega) < 0$ hold, then the state $\boldsymbol{X}_+^*$ with the designed k and T is stable for any $a \in (0, a_g]$, any topology $\boldsymbol{L}$, and any coupling strength $\varepsilon > 0$.

C. Numerical examples

In this subsection, we confirm the validity of our analytical results through numerical simulations. Let us fix the parameter $b = 0.2$ throughout this subsection. For a stand-alone bus system, an increase in parameter a destabilizes the stable fixed point $\boldsymbol{p}_+$ at $a = a_{\mathrm{HP}} = 5/36$ via the Hopf bifurcation, and then $\boldsymbol{p}_+$ vanishes at $a = a_{\mathrm{SN}} = 1/4$ via the saddle-node bifurcation [16]. We now focus on the unstable fixed point $\boldsymbol{p}_+$ at $a = a_g \equiv 0.17 \in [a_{\mathrm{HP}}, a_{\mathrm{SN}}]$.

The controller parameters k and T are now designed in accordance with the above steps. Step 1: The parameters $a = a_g \equiv 0.17$ and $b = 0.20$ are given. Step 2: We confirm that assumption (19), i.e., $0.20 < 0.2774 < 1$, holds. The parameters, $a = 0.17, a^* = 0.2774$, and $b = 0.20$ are substituted into inequalities (20), and then the polynomials $d_{1,2,3}$ have only k as a variable. The stable intervals of T are obtained from Eq. (21) if inequalities (20) hold (see Fig. 9). The gray regions are the parameter sets in which $g(s,T,0)$ is stable. We set $(k,T) = (0.10, 5.00)$ [16]. Step 3: $f_1(\omega)$ and $f_2(\omega)$ with $(k,T) = (0.10, 5.00)$ are plotted in Fig. 10. Note that $f_1(\omega) = 0$ has an unique root (i.e., • in Fig. 10), but the root does satisfy $f_2(\omega) < 0$. As a result, we can guarantee that $\boldsymbol{X}_+^*$ with $(k,T) = (0.10, 5.00)$ is stable for any $a \in (0, 0.17]$, any topology $\boldsymbol{L}$, and any coupling strength $\varepsilon > 0$.

Now we consider the same situation as in Fig. 3, except that $a = 0.17$. Figure 11 shows the time-series data of x_n, $u_n^{(\varepsilon)}$, and $u_n^{(k)}$ on the switched bus network with decentralized delayed-feedback controller (14). All of the states x_n are stabilized on $x_+^* = 0.7828$, and all of the connection signals $u_n^{(\varepsilon)}$ and the control signals $u_n^{(k)}$ converge on 0. This numerical result indicates that controller (14) designed as described in the above steps works well in the numerical simulations.

Let us investigate the dynamic behavior of the controlled bus network with parameter mismatch. We now consider situation (a) in Sec. II C. The parameters, a_n, b_n, and ε_n, are

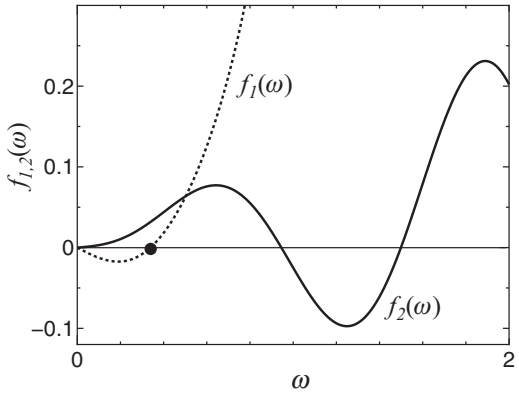

FIG. 10. Functions $f_1(\omega)$ and $f_2(\omega)$ plotted with respect to $\omega > 0$ for designed $(k,T) = (0.10, 5.00)$ ($a = 0.17, b = 0.20$). There exists no ω such that both $f_1(\omega) = 0$ and $f_2(\omega) < 0$ hold.

randomly chosen with nominal values, $\bar{a} = 0.17$, $\bar{b} = 0.20$, and $\bar{\varepsilon} = 0.1$ or 1.0, and with $p = 0.1$ (10% error). As shown in Fig. 12, the states x_n are stabilized in the spatially nonuniform equilibrium state. In contrast, all of the control signals $u_n^{(k)}$ converge on 0 due to its noninvasive property. We may conclude that decentralized delayed-feedback controller (14) is robust against parameter mismatch.

Here we focus on the situation in which bus system 1 has a slow time-varying CPL, $a_1 = 0.17 + 0.15 \sin 2\pi(\tau - 100)/400$, and the other systems have a constant CPL, $a_2 = \cdots = a_5 = 0.17$, on the bus system network shown in Fig. 5 with decentralized delayed-feedback controller (14). The other parameters are fixed at $b_1 = \cdots = b_5 = 0.2$ and $\varepsilon = 1.0$. Bus system 1 is connected to bus systems 2 and 3. Figure 13 shows the behavior of the bus network. Parameter a_1 is fixed at $a_1 = 0.17$ until $\tau = 100$ and varies from $\tau = 100$. Since parameter a_1 varies with large amplitude, it often exceeds a_{SN}, where a stand-alone bus system 1 has no fixed

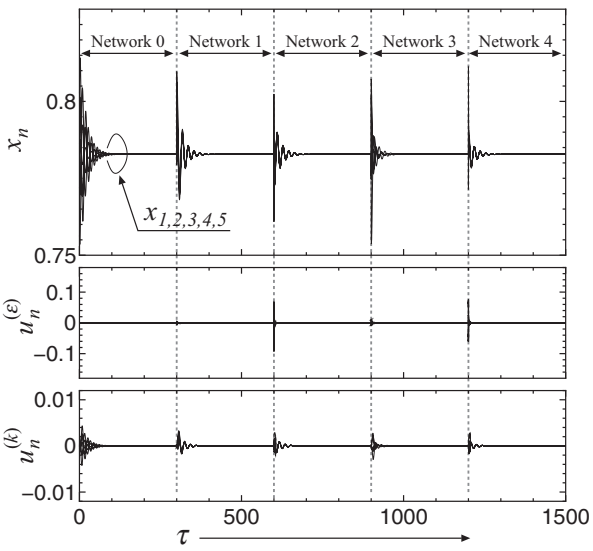

FIG. 11. Time-series data of x_n, $u_n^{(\varepsilon)}$, $u_n^{(k)}$ $(n = 1, \ldots, 5)$ of the switched bus network ($a = 0.17, b = 0.20$) with decentralized delayed-feedback controller (14) ($k = 0.10, T = 5.00$). The situation is the same as in Fig. 3, except that $a : 0.10 \to 0.17$ and $k : 0 \to 0.10$.

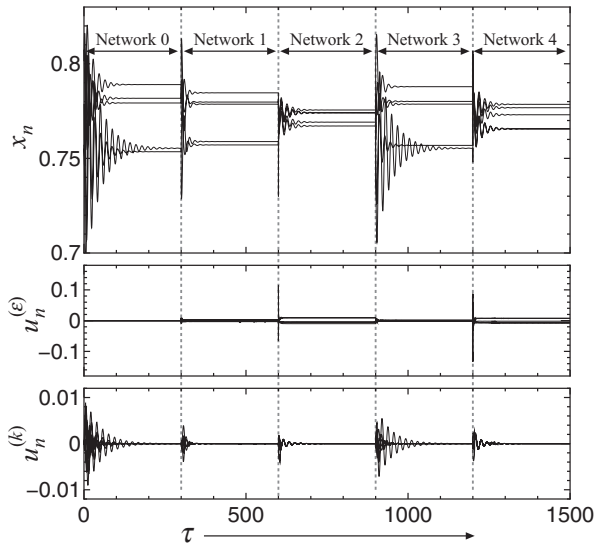

FIG. 12. Time-series data of x_n, $u_n^{(\varepsilon)}$, $u_n^{(k)}$ $(n = 1,\ldots,5)$ of the switched bus network ($\bar{a} = 0.17$, $\bar{b} = 0.20$, $\bar{\varepsilon} = 0.1$ or 1.0) with parameter mismatch $p = 0.1$ (10% error). The situation is the same as in Fig. 11, except for parameter mismatch.

point. In addition, the other parameters $a_2 = \cdots = a_5 = 0.17$ exceed a_{HP}, where a stand-alone bus system has the unstable fixed point $\boldsymbol{p}_+$. Despite such a severe situation, controller (14) traps the wandering spatially nonuniform state with a small control signal.

Let us summarize the numerical results. The decentralized delayed-feedback controller designed using our systematic procedure enhances the stability of the spatially uniform equilibrium state in bus networks. The controller enhances the stability of the spatially *nonuniform* equilibrium state

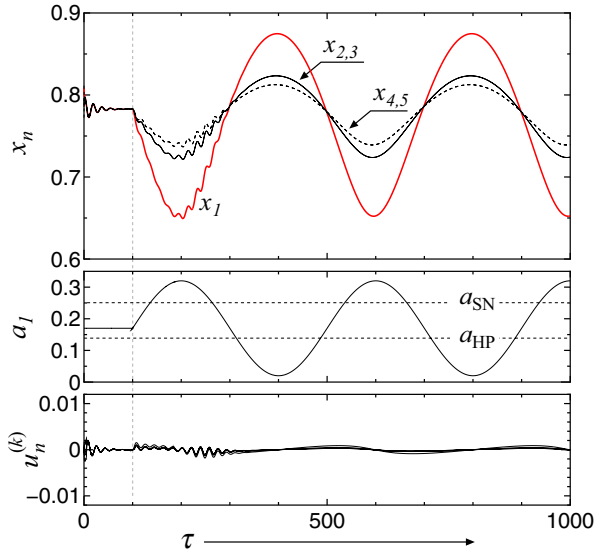

FIG. 13. (Color online) Time-series data of x_n, a_1, and $u_n^{(k)}$ $(n = 1,\ldots,5)$ of the controlled bus network ($k = 0.10, T = 5.00$), with a slow time-varying CPL $a_1 = 0.17 + 0.15\sin 2\pi(\tau - 100)/400$, shown in Fig. 5. Bus system 1 is connected to bus systems 2 and 3.

with parameter mismatch. The controller tracks the spatially *nonuniform* equilibrium state with a slow time-varying CPL. These results indicate that the controller has two advantages. First, since control law (14) does not use information about the equilibrium state, there is no need to obtain accurate values of the system parameters. This is a useful advantage for the practical situation in which there is a lack of accurate information on bus systems. Second, controller (14) consumes only a small amount of control energy for stabilizing or tracking states due to its noninvasive property. This advantage may allow us to implement controller (14) with a small size and a low cost.

IV. DISCUSSION

We now review previous studies related to the results of the present study. Huddy and Skufca reported that delay connections can induce the stabilization of an operating point in coupled dc bus systems [22]. This stabilization is referred to as time-delay-induced amplitude death, which is a well-known phenomenon in the field of nonlinear science [31–34]. The stability of amplitude death is closely related to that of our decentralized delayed-feedback controller (14). The delay connections for amplitude death can be realized by replacing x_m with $x_{m,T}$ in connection signal (4); thus, the characteristic quasipolynomial describing the stability of uniform equilibrium state $\boldsymbol{X}_+^*$ differs from quasipolynomial (17). However, it should be noted that these quasipolynomials have a common term $g(s,T,0)$. This term, dealt with in Theorem 2, describes the stability of the fixed point $\boldsymbol{p}_+$ in a stand-alone bus system controlled by delayed feedback [16]. Therefore, we notice that the stability of $\boldsymbol{p}_+$ with delayed feedback is a necessary condition for stability of $\boldsymbol{X}_+^*$ with the delay connection and that with the decentralized delayed feedback. Furthermore, one of the most interesting common features of the time-delay-induced amplitude death and the decentralized delayed-feedback control is that the time delay, which is considered to be a destabilizing factor in the field of control theory, is used as a stabilizing factor.

It is well known that the tracking filter, which is implemented simply by RC in electronic circuits, can stabilize unstable fixed points in stand-alone nonlinear systems [28,35]. This filter has been used for stabilization of an operating point in stand-alone dc bus systems [7]. On the other hand, a simple method for increasing capacitance C and that for connecting an additional capacitor in parallel with C have been widely used for such stabilization [9]. However, these methods tend to require large capacitors, which are generally big, heavy, and expensive. Therefore, they would not be suitable for industrial applications with severe restrictions on space, weight, or cost. In contrast, the decentralized delayed-feedback control does not require large capacitors.

V. CONCLUSION

The present paper extended our previous study [16] to bus networks. The stability of the operating point in a stand-alone dc bus system is equivalent to that in networks for any network topology and any coupling strength. The delayed-feedback control was applied to every bus system, and an unstable operating point embedded within the network was

then stabilized. The controller parameters were systematically designed based on stability analysis. Numerical simulations were conducted in order to demonstrate the robustness of the bus system networks with respect to parameter mismatch and a slow-varying parameter.

ACKNOWLEDGMENTS

The present study was supported in part by JSPS KAKENHI (26289131) and by the Research Foundation for the Electrotechnology of Chubu.

[1] Y. Susuki and I. Mezic, IEEE Trans. Power Sys. **26**, 1894 (2011).
[2] Y. Takatsuji, Y. Susuki, and T. Hikihara, Nonlin. Theor. Appl. **2**, 347 (2011).
[3] F. Dorfler, M. Chertkov, and F. Bullo, Proc. Natl. Acad. Sci. U.S.A. **110**, 2005 (2013).
[4] A. Motter, S. Myers, M. Anghel, and T. Nishikawa, Nat. Phys. **9**, 191 (2013).
[5] P. Menck, J. Heitzig, J. Kurths, and H. Schellnhuber, Nat. Commun. **5**, 3969 (2014).
[6] J. J. Justo, F. Mwasilu, J. Lee, and J.-W. Jung, Renew. Sust. Energ. Rev. **24**, 387 (2013).
[7] M. Cespedes, L. Xing, and J. Sun, IEEE Trans. Power Elect. **26**, 1832 (2011).
[8] A. Griffo, J. Wang, and D. Howe, in *Proc. of IEEE Vehicle Power and Propulsion Conference* (IEEE, Harbin, China, 2008).
[9] A. Kwasinski and C. Onwuchekwa, IEEE Trans. Power Elect. **26**, 822 (2011).
[10] X. Liu, Y. Zhou, W. Zhang, and S. Ma, IEEE Trans. Vehicular Techn. **60**, 2042 (2011).
[11] K. Inoue, T. Kato, M. Inoue, Y. Moriyama, and K. Nishii, in *Proc. of 2012 IEEE 13th Workshop on Control and Modeling for Power Electronics* (IEEE, Kyoto, Japan, 2012).
[12] H. Mosskull, Control Eng. Pract. **27**, 61 (2014).
[13] G. Sulligoi, D. Bosich, G. Giadrossi, L. Zhu, M. Cupelli, and A. Monti, IEEE Trans. Smart Grid **5**, 2543 (2014).
[14] W.-J. Lee and S.-K. Sul, IEEE Trans. Indust. Appl. **50**, 404 (2014).
[15] Y. Zhao, W. Qiao, and D. Ha, IEEE Trans. Indust. Appl. **50**, 1448 (2014).
[16] K. Konishi, Y. Sugitani, and N. Hara, Phys. Rev. E **89**, 022906 (2014).
[17] K. Pyragas, Phys. Lett. A **170**, 421 (1992).
[18] A. Radwan and Y.-R. Mohamed, IEEE Trans. Smart Grid **3**, 203 (2012).
[19] E. Jamshidpour, B. Nahid-Mobarakeh, P. Poure, S. Pierfederici, F. Meibody-Tabar, and S. Saadate, IEEE Trans. Power Elect. **28**, 1833 (2013).
[20] S. Anand and B. Fernandes, IEEE Trans. Indust. Elect. **60**, 5040 (2013).
[21] P. Magne, B. Nahid-Mobarakeh, and S. Pierfederici, IEEE Trans. Indust. Appl. **49**, 2352 (2013).
[22] S. Huddy and J. Skufca, IEEE Trans. Power Elect. **28**, 247 (2013).
[23] K. Konishi, Int. J. Bifurcat. Chaos **20**, 3351 (2010).
[24] R. Merris, Lin. Algebr. Appl. **197-198**, 143 (1994).
[25] K. Pyragas, Phil. Trans. R. Soc. A **364**, 2309 (2006).
[26] E. W. Hooton and A. Amann, Phys. Rev. Lett. **109**, 154101 (2012).
[27] K. Pyragas and V. Novicenko, Phys. Rev. E **88**, 012903 (2013).
[28] A. Namajūnas, K. Pyragas, and A. Tamaševičius, Phys. Lett. A **204**, 255 (1995).
[29] A. Gjurchinovski, T. Jüngling, V. Urumov, and E. Schöll, Phys. Rev. E **88**, 032912 (2013).
[30] H. Kokame, K. Hirata, K. Konishi, and T. Mori, Int. J, Control **74**, 537 (2001).
[31] D. V. Ramana Reddy, A. Sen, and G. L. Johnston, Phys. Rev. Lett. **80**, 5109 (1998).
[32] G. Saxena, A. Prasad, and R. Ramaswamy, Phys. Rep. **521**, 205 (2012).
[33] A. Koseska, E. Volkov, and J. Kurths, Phys. Rep. **531**, 173 (2013).
[34] Y. Sugitani, K. Konishi, L. B. Le, and N. Hara, Chaos **24**, 043105 (2014).
[35] N. F. Rulkov, L. S. Tsimring, and H. D. I. Abarbanel, Phys. Rev. E **50**, 314 (1994).